Resonant waveguide device with vertical gratings

Hyo-Chang Kim, Kazuhiro Ikeda, and Yeshaiahu Fainman

Department of Electrical and Computer Engineering, University of California, San Diego, 9500 Gilman Drive, La Jolla, California 92093-0407

Received August 4, 2006; revised November 10, 2006; accepted November 17, 2006; posted December 4, 2006 (Doc. ID 73794); published February 2, 2007

Transmission resonant filters in a waveguide with vertical gratings have been realized in silicon on insulator wafers. Experimental studies of fabricated devices show a broad stopband of ~19 nm in the center of which exists a narrow transmission band of ~0.5 nm with a quality factor of ~3000. These resonant cavities are useful for laser cavities, switches, modulators, detectors, and tunable filters. © 2007 Optical Society of America

OCIS codes: 230.1480, 230.5750, 230.7400, 230.3120.

The distributed Bragg reflector (DBR) in planar waveguide technology has been used to perform and enhance various functionalities of optical elements such as single-mode selectors in semiconductor lasers, optical filters, switches, modulators, couplers, detectors, and sensors.[1–5] A DBR structure exhibits in its transmission spectrum a stopband centered at the Bragg wavelength, where the bandwidth of the stopband is determined by the amplitude of the periodic index modulation and the Bragg wavelength is determined by the mean period of the index modulation. Many devices use a quarter-wavelength phase shift embedded in the middle of a DBR structure to construct a highly resonant cavity and create a narrow resonant transmission band in the middle of the stopband at the Bragg wavelength.[2,4,5] The DBRs conventionally fabricated on the surface of the waveguide involve an additional procedure separate from the waveguide.[1–5] In contrast, we exploit a method to define the DBRs and nanostructured resonant devices by using corrugation of waveguide sidewalls. This method was first developed to create periodic corrugations of single-mode distributed feedback lasers and distributed reflector lasers.[6–8] In this Letter, we extend this approach to implement passive transmission resonant filters by using a silicon on insulator (SOI) material system.

We consider the schematic structure of the resonant transmission filter, where vertical gratings with full depth of single side (ΔW_S) are engraved on both sidewalls of the waveguide with the average width (W_S). It is assumed that a 250-nm-thick silicon core is surrounded by silicon dioxide. A pair of Bragg reflectors each of length (L) and period (Λ) is separated by a half-period ($\Lambda/2$). For the transverse electric (TE) fundamental mode, where the electric field is parallel to the wafer surface, the coupling coefficient (κ) for the first-order vertical grating is given by[3]

$$\kappa = \Gamma\left(\frac{\pi}{\lambda}\frac{\Delta W_S}{W_{eff}}\frac{n_S^2 - n^2}{nq}\right)\left[\frac{n^2}{n_S^2} - \frac{n^2}{n_{\mathrm{SiO}_2}^2} + 1\right], \qquad (1)$$

where $n \equiv \beta/k$ is the effective index of the guided mode with the propagation constant β and the wavenumber in vacuum k; n_S is the effective index of the symmetric slab waveguide,[9] where the refractive indices of the silicon core layer and silicon dioxide cladding layers (n_{SiO_2}) are assumed to be 3.5 and 1.4, respectively; Γ is a fraction of the TE mode confined in the silicon core (~85% for this study)[10]; $q \equiv (n/n_S)^2 + (n/n_{\mathrm{SiO}_2})^2 - 1$; and effective width $W_{eff} \equiv W_S + 2/(q\gamma)$ with $\gamma \equiv (\beta^2 - k^2 n_{\mathrm{SiO}_2}{}^2)^{1/2}$. Equation (1) indicates that κ is linear in ΔW_S, whereas the corresponding Bragg length ($L_B = 1/\kappa$) is inversely proportional to ΔW_S. We construct a resonant waveguide of $W_S = 500$ nm with values of $\Delta W_S = 50$, 75, 100 nm, corresponding to κ of ~600, 900, and 1200 cm^{-1} at $\lambda = 1550$ nm.

Next, consider a Fabry–Perot (FP) type filter made from a pair of such identical Bragg reflectors, each having reflection (r) and transmission amplitude (t) coefficients and separated by a spacer of length $d = \Lambda/2$, causing a phase shift ($\phi = \pi/2$). The transmission amplitude of the resonant filter (t_{RF}) as a function of λ is given by

$$t_{RF} = \frac{t^2 \exp(i\phi)}{1 - r^2 \exp(2i\phi)}, \qquad (2)$$

where $t = 1/\{\cosh(\mu L) - (i\delta - \alpha/2)[\sinh(\mu L)]/\mu\}$, $r = -i\kappa t[\sinh(\mu L)]/\mu$, $\mu^2 \equiv \kappa^2 + (i\delta - \alpha/2)^2$ with detuning parameter $\delta \equiv \beta - \beta_B \sim (\mathrm{d}\beta/\mathrm{d}\omega)(\omega - \omega_B) = (\omega - \omega_B)/v_g$, α is the loss of Bragg reflector, ω is the angular frequency, ω_B ($\equiv 2\pi c/\lambda_B$) is the Bragg angular frequency, v_g ($\equiv c/n_g$) is the group velocity of the waveguide mode, c is the speed of light in vaccum, λ_B ($\equiv 2n\Lambda$) is the Bragg wavelength, and n_g [$= n - \lambda_B(\Delta n/\Delta\lambda)$] is the group index of the waveguide mode.[2,5] Figure 1 shows the simulated results of transmitted power, $|t_{RF}|^2$, as a function of the deviation from λ_B. In the simulation, we used $n_g = 3.8$ and κ values calculated at $\lambda_B = 1550$ nm. We determined the value of $n_g = 3.8 \pm 0.1$ by measuring FP resonant mode spacing of a straight waveguide with $W_S = 500$ nm at $\lambda = 1550$ nm. The black, blue, and red lines correspond to $\kappa = 600$, 900, and 1200 cm^{-1}; $\alpha = 10$, 20, and 30 cm^{-1}; and $L = 70\ \mu\mathrm{m}$ ($2.1 \times L_B$), 50 μm ($2.25 \times L_B$), and 40 μm ($2.4 \times L_B$), respectively.

The designed devices are fabricated on a ~0.5 cm^2 size of 15.24 cm SOI wafer consisting of a silicon top layer with a mean thickness of 252.2 nm with a distribution of $6\sigma \sim 18.3$ nm on a ~3-μm-thick silicon di-

0146-9592/07/050539-3/$15.00

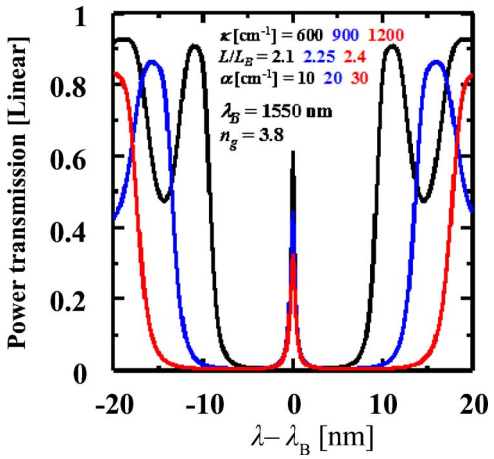

Fig. 1. (Color online) Simulated plots of transmitted power from the devices.

oxide layer. Polymethylmethacrylate with 950 K molecular weight is spin-coated on the sample and baked, resulting in ~200 nm thickness. A scanning electron microscope (SEM) equipped with a 16 bit digital-to-analog converter and pattern generation software is used to pattern the whole structure at an acceleration voltage of 40 kV. Following a standard lift-off process using ~20-nm-thick nickel, the silicon layer is selectively etched in a reactive ion etcher using a mixture of BCl_3/Ar with the following conditions: gas flow rates BCl_3/Ar=10/10 SCCM, pressure ~30 mTorr, power density ~0.1 W/cm^2, and temperature ~20°C. This results in an etching rate of ~75 nm/min for a sample size of ~1×0.5 cm^2. The choice of a BCl_3/Ar mixture enables us to use the buried oxide layer as an etching stop layer. After chemically removing nickel, an ~1-μm-thick buffer layer of silicon dioxide is sputtered on the whole structure. After cleaving of the facets of the device, an antireflection coating (Si_3N_4) is sputtered to reduce additional FP resonance due to the cleaved facets. A tilted SEM image of the fabricated vertical grating is shown in Fig. 2(a). Magnified views are displayed in the insets of Fig. 2(a).

Optical power should be delivered from the fiber to the filters. Our SEM-based lithography system has only 90×90 μm^2 of writing area, with resolution sufficient for patterning of the vertical gratings. It is well known that, when the waveguide width is tapered or expanded over a certain length, its guided mode also changes adiabatically. The adiabatic mode matching can be used to transfer a tightly confined waveguide mode to a larger size mode for efficient coupling with optical fiber.[11,12] Here, we apply this concept for interconnection of waveguides patterned at different magnifications. In a 90×90 μm^2 area, the remaining length of ~20 μm from the longest filter length of 70 μm is assigned to expand the width from 500 nm to 1.5 μm in each end (~10 μm). Without moving the sample and changing other microscope settings, we first fabricate the patterns in a 90 μm^2 writing area at 1000× magnification and then 2 μm wide waveguides in 300×300 μm^2 at 300×. Pattern displacements at the boundaries of the two writing areas are measured from SEM inspections. The displacements are then corrected by shifting the design of 2 μm wide waveguide patterns. We have empirically found that ~200 nm placement accuracy can be routinely obtained without repetitions. Figure 2(b) shows a micrograph of the whole device, and the inset shows the magnified view of the tapered waveguide connections.

For testing, a TE-polarized tunable laser source is coupled into polarization-maintaining tapered fiber with an output spot diameter of ~2.5 μm, producing ~20 dB polarization extinction. Another polarization-maintaining tapered fiber is used to collect light from the fabricated devices and its relative power transmission over the wavelength is analyzed. Figure 3 shows the measured transmission spectra, which are in good agreement with the calculated prediction shown in Fig. 1. Oscillatory behavior outside of the stopband and a slight asymmetry of the resonant transmission band are most likely due to residual reflections on the two Si_3N_4-coated facets. Comparison of Figs. 1 and 3(a) indicates that Eq. (1) along with Eq. (2) predicts the result with good accuracy in $\Delta W_S/W_S=10\%$. Comparison of Figs. 1 and 3(b) shows that as $\Delta W_S/W_S>10\%$, Eq. (1) tends to start overes-

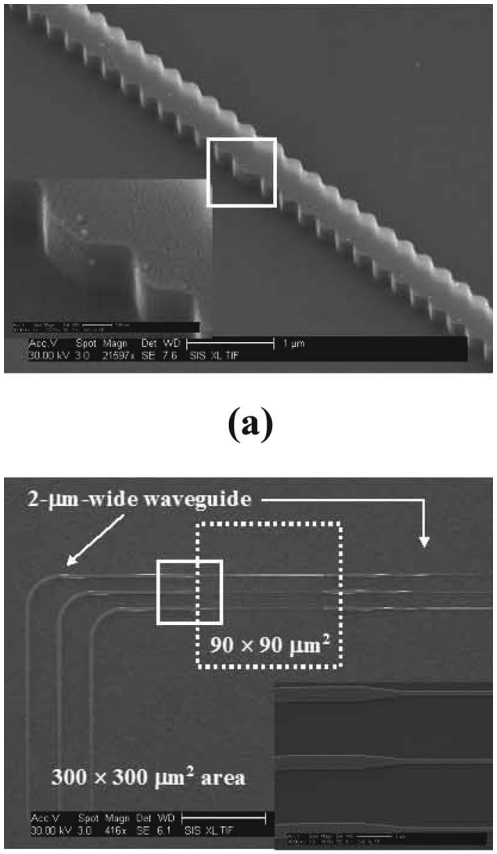

Fig. 2. SEM micrographs of the devices. The insets show magnified views of the rectangles: (a) Transmission resonant filter with vertical gratings. (b) Micrograph of the whole device and its inset showing the waveguide connection defined at two different magnifications. The dotted rectangle shows the area defined at 1000× magnification.

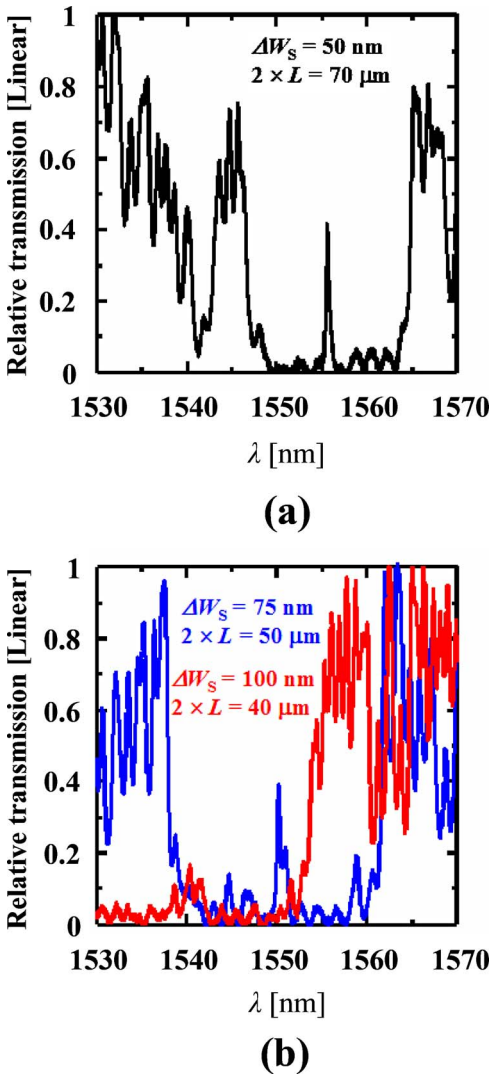

Fig. 3. (Color online) Measured transmission spectra from the fabricated devices designed in Fig. 1 with $W_S = 500$ nm and $\Lambda = 305$ nm for (a) $\Delta W_S = 50$ nm, $2 \times L = 70$ μm and (b) blue curve, $\Delta W_S = 75$ nm, $2 \times L = 50$ μm; red curve, $\Delta W_S = 100$ nm, $2 \times L = 40$ μm.

timating κ and the corresponding λ_B also starts to shift toward shorter wavelength as ΔW_S is increased. Although W_S (=500 nm) determines λ_B in Eq. (1) and (2), the effective width becomes narrower as ΔW_S increases due to the large index difference between Si and SiO_2.

In summary, passive transmission resonant filters with vertical gratings on an SOI wafer have been realized for what is believed to be the first time. Bragg reflectors are constructed by engraving vertical gratings with 10–20% modulation depth of their waveguide width on both sidewalls of a 500-nm-wide waveguide. Transmission resonant filters are created by introducing a half-period offset into a pair of Bragg reflectors with vertical gratings. The measured transmission spectrum of the fabricated device shows a wide stopband of ~19 nm, in the center of which exists a narrow transmission band of ~0.5 nm with a quality factor $Q \sim \lambda_B/\Delta\lambda \sim 3000$.

The authors thank A. Krishnamoorthy and J. Cunningham at Sun Microsystems for valuable suggestions and encouragement, and B. R. Henry at Trion Technology for suggesting their silicon etching with $BCl_3/Cl_2/Ar$ mixtures. Financial support from the National Science Foundation, the Air Force Office of Scientific Research, and the Defense Advanced Research Projects Agency is gratefully acknowledged. K. Ikeda acknowledges receiving a scholarship from the Nakajima Foundation, Japan. H.-C. Kim's e-mail address is hckim@emerald.ucsd.edu.

References

1. H. Kogelnik, in *Integrated Optics*, Vol. 7 of Topics in Applied Physics, T. Tamir, ed. (Springer-Verlag, 1979), pp. 13–81.
2. H. A. Haus, *Waves and Fields in Optoelectronics* (Prentice-Hall, 1984), pp. 235–253.
3. D. G. Hall, in *Progress in Optics*, E. Wolf, ed. (North-Holland, 1991), Vol. XXIX, pp. 1–63.
4. Y. Suematsu and A. R. Adams, *Handbook of Semiconductor Lasers and Photonic Integrated Circuits* (Chapman & Hall, 1994).
5. C. H. Henry, Y. Shani, R. C. Kisler, T. E. Jewell, V. Pol, N. A. Olsson, R. F. Kazarinov, and K. J. Orlowski, J. Lightwave Technol. **7**, 1379 (1989).
6. J. Wiedmann, K. Ebihara, H. C. Kim, B. Chen, M. Ohta, K. Matsui, S. Tamura, J.-I. Shim, and S. Arai, Electron. Lett. **37**, 831 (2001).
7. H. C. Kim, J. Wiedmann, K. Matsui, S. Tamura, and S. Arai, Jpn. J. Appl. Phys. **40**, L1107 (2001).
8. H. C. Kim, H. Kanjo, T. Hasegawa, S. Tamura, and S. Arai, IEEE J. Sel. Top. Quantum Electron. **9**, 1146 (2003).
9. D. Marcuse, *Theory of Dielectric Optical Waveguides*, 2nd ed. (Academic, 1991), pp. 1–14.
10. G. P. Agrawal and N. K. Dutta, IEEE J. Quantum Electron. **21**, 534 (1985).
11. Y. Shani, C. H. Henry, R. C. Kistler, K. J. Orlowsky, and D. A. Ackerman, Appl. Phys. Lett. **55**, 2389 (1989).
12. T. Shoji, T. Tsuchizawa, T. Watanabe, K. Yamada, and H. Morita, Electron. Lett. **38**, 1669 (2002).